International Journal of Heat and Mass Transfer 53 (2010) 1308–1312

Contents lists available at ScienceDirect

International Journal of Heat and Mass Transfer

journal homepage: www.elsevier.com/locate/ijhmt

Ab initio calculations of thermal radiative properties: The semiconductor GaAs

Hua Bao, Xiulin Ruan *

School of Mechanical Engineering, Birck Nanotechnology Center, and Energy Center, Purdue University, West Lafayette, IN 47907-2088, USA

ARTICLE INFO

Article history:
Received 24 August 2009
Received in revised form 12 December 2009
Available online 7 January 2010

Keywords:
GaAs
Radiation
Ab initio Calculation

ABSTRACT

Spectral reflectance of GaAs from infrared (IR) to ultra-violet (UV) bands is predicted using ab initio calculations. We first predict the spectral dielectric function. Two major mechanisms exist for different photon wavelength, namely, photon–electron coupling in the UV to near-IR region and photon–phonon coupling in the far-IR region. For the near-IR to UV band, the electronic band structure of GaAs is calculated, and the imaginary part of the dielectric function is determined from the band structure using the Fermi's golden rule. The real part of spectral dielectric function is then derived from Kramer–Kronig transformation. For the far-IR region, ab initio calculations are used to determine the phonon modes, and the dielectric function is then predicted using the oscillator model. The spectral reflectance for the entire spectrum is then calculated using Fresnel's law for a semi-infinite GaAs slab. The predicted results agree reasonably well with experimental data, demonstrating the capability of ab initio calculations to predict thermal radiative properties of semiconductor materials from their atomic structures.

1. Introduction

It is desirable to control the spectrum and direction of thermal emission in a broad set of thermal management and energy conversion applications, such as in aerospace [1], solar cells [2], thermophotovoltaics [3,4], optical filters, etc. Selective emission properties can be pursued at multiple scales, expanding from atomic scale to macroscale. Recently, nanostructures have been investigated extensively for their interesting radiative properties, such as antenna effects [5], photonic band gap [6], and wavelength-selective emission [7]. On the other hand, bulk materials have received much less attention. Actually, many bulk materials, such as rare-earth oxides [8], also exhibit selective radiative properties due to their special atomic structures. Understanding the relationship between the atomic structure and the macroscopic radiative property can be crucial for designing new bulk materials with desired selective radiative properties, and can offer more design space in addition to making them into various nanostructures.

The fundamental macroscopic material property that determines radiative properties is the dielectric function, which describes the response of a material to a time-dependent external electromagnetic (EM) field. The response to external field (or photons) from far-IR to UV band can be attributed to different mechanisms, including impurity, optical phonon, free carrier, exciton, and interband electronic transition. The relative importance of each mechanism depends on wavelength and material. For example, free electrons dominate the dielectric response in metals almost at all wave length [9]. In contrast, in semiconductors like GaAs studied here, the dominating mechanisms are electronic transitions in the visible band (strictly speaking, from band gap energy to UV band) and optical phonon absorption in the far-IR band. Several dielectric function models are developed to account for different mechanisms, such as Drude's model for free electrons and Lorentz oscillator model for phonons [9]. However, the parameters in these models are typically obtained from experiments, limiting their applications in predicting radiative properties from atomic structures especially for new materials where experimental data are not available.

With the rapid progress of ab initio methods, the dielectric function models may now be parameterized using ab initio calculations. As such, the relationship between the atomic structure and their radiative properties can be understood using a multiscale simulation approach including ab initio calculations and EM wave theory. Density functional theory (DFT) is a typical ab initio method. Given the initial unit cell structure, it can predict many material properties with a reasonable accuracy, such as equilibrium material structure, electronic band structure, and phonon properties. These results can be used in the dielectric function models to calculate the frequency-dependent dielectric function. EM theory can then be used to calculate radiative properties of bulk materials and nanostructures including photonic crystals, nanoantennas, nanoparticles, etc.

In this work, we demonstrate the capacity of a combination of ab initio calculations and EM theory to predict radiative properties from atomic structures, using GaAs as an example. We first use ab initio calculations to predict the dielectric function at different wavelength regimes. For visible bands, the electronic structure is

* Corresponding author. Tel.: +1 765 494 5721; fax: +1 765 494 0539.
E-mail address: ruan@purdue.edu (X. Ruan).

0017-9310/$ - see front matter © 2009 Elsevier Ltd. All rights reserved.
doi:10.1016/j.ijheatmasstransfer.2009.12.033

Nomenclature

D	electric displacement
E	electric field
$\mathbf{k}$	wave vector
m	mass, complex refractive index
n	real part of refractive index
p	momentum operator
R	reflectance
T	transmittance
$\mathbf{r}$	position vector
V	potential energy
w	weight of a k-point
x	x-coordinate

Greek symbols

κ	imaginary part of refractive index
Γ	smearing factor
γ	damping factor
φ	wave function
ε	eigen energy
ρ	charge density
ϵ'	real part of dielectric function
ϵ''	imaginary part of dielectric function
δ	delta function
Ω	unit-cell volume
ω	angular frequency

Subscripts and superscripts

0	ground state, static
ext	external
i, j	numerical index
KS	Kohn–Sham
LO, TO	longitudinal optical, transverse optical (phonon)
mac	macroscopic
m, n	numerical index
v	valence
∞	infinity
a, b	direction index

calculated, and the transition probabilities are determined using the Fermi's golden rule [10]. Then imaginary and real parts of the dielectric function from the near-IR to UV band are predicted. For far-IR bands, the vibrational eigen energies (phonon frequencies) and eigen displacements are calculated from first principles. By analyzing the symmetry of each vibrational mode using normal mode analysis [11], the IR-active phonon modes are identified. The dielectric function in IR band is predicted using the oscillator model. Combining the dielectric functions due to electronic and phonon absorptions, the reflectance over the entire spectrum for bulk GaAs is calculate and compared with experimental data.

2. Theory and methods

2.1. Density functional theory

DFT is a quantum mechanical theory to investigate the ground state of many-body systems. In the framework of DFT, many-body systems are treated as systems of interacting electrons in an external potential $V_{\text{ext}}(\mathbf{r})$. The ground state energy of the system is completely determined given the ground state electron density $\rho_0(\mathbf{r})$ only. A functional $E[\rho]$ for the ground state energy can be defined in terms of $\rho(\mathbf{r})$. For a particular $V_{\text{ext}}(\mathbf{r})$, the exact ground state energy of the system is the global minimum value of this functional, and the $\rho(\mathbf{r})$ that minimizes the functional is the exact ground state density $\rho_0(\mathbf{r})$ [12]. Kohn–Sham (KS) approach further replaces the difficult interacting many-body system with an independent particle system. The single particle KS equations are [13]

$$\left[-\frac{\hbar^2\nabla^2}{2m}+V_{\text{KS}}(\mathbf{r})\right]\varphi_{n\mathbf{k}}(\mathbf{r})=\varepsilon_{n\mathbf{k}}\varphi_{n\mathbf{k}}(\mathbf{r}), \tag{1}$$

with a local effective potential $V_{\text{KS}}(\mathbf{r})$, where m is the mass of the electron, φ is wave function, and ε is the eigen energy. In a periodic solid where the wave vector $\mathbf{k}$ is a good quantum number, the KS orbitals $\varphi_{n\mathbf{k}}(\mathbf{r})$ are Bloch states with band index n, wave vector $\mathbf{k}$, and energy $\varepsilon_{n\mathbf{k}}$. The ground state density $\rho(\mathbf{r})$ can be represented by the wave functions using

$$\rho(\mathbf{r})=2\sum_{v\mathbf{k}}|\varphi_{v\mathbf{k}}(\mathbf{r})|^2, \tag{2}$$

where v donates the summation of the valence bands. $V_{\text{KS}}(\mathbf{r})$ is given by

$$V_{\text{KS}}(\mathbf{r})=V_{\text{ext}}(\mathbf{r})+V_{\text{H}}(\mathbf{r})+V_{\text{xc}}(\mathbf{r}). \tag{3}$$

Here V_{ext} is the external potential, which is usually the ion–electron interaction potential and can be replaced by a pseudopotential. $V_{\text{H}}(\mathbf{r})$ is the Hartree potential, which is simply the Coulomb interaction between electrons and can be determined by electron density $\rho(\mathbf{r})$. $V_{\text{xc}}(\mathbf{r})$ is the exchange and correlation potential, which contains many complicated terms, including quantum electron repulsion, electron kinetic energy, electron correlation energy, etc. Many functionals are available to predict the exchange and correlation energy from electron density. Once the KS potential energy is determined, those single particle KS equations can be solved by iterative minimization or other advanced algorithms [14].

2.2. Spectral dielectric function at optical frequencies

Electronic interband transitions dominate the photon absorption at near-IR, visible, and UV bands. The transition probability is determined by the transition matrix elements $p^a_{ij}=\langle\mathbf{k}i|p_a|\mathbf{k}j\rangle$ [15], where $\langle\mathbf{k}i|$ and $|\mathbf{k}j\rangle$ are wave functions of the initial and final states and p_a is in general the operator which couples the initial and final states. In this case, p_a is the momentum operator. With an integration of transition matrix elements over all the possible vertical transitions across the band gap, the imaginary part of the dielectric function $\epsilon(\omega)$ can be determined by the Fermi's golden rule (in atomic units) [16],

$$\epsilon''_{a,a}(\omega)=\frac{4\pi^2}{\Omega\omega^2}\sum_{i\in\text{VB},j\in\text{CB}}\sum_{\mathbf{k}}w_{\mathbf{k}}\left|p^a_{ij}\right|^2\delta(\epsilon_{\mathbf{k}j}-\epsilon_{\mathbf{k}i}-\omega), \tag{4}$$

where Ω is the unit-cell volume and ω is photon frequency, VB and CB denote the valence and conduction bands, $w_{\mathbf{k}}$ is the weight associated with a k-point, and a denotes a particular direction. The delta function is used to ensure the energy conservation associated with an electronic transition: only when the photon energy matches the energy difference between a valence and conduction state, the transition can occur. Dirac delta function $\delta(x)$ can be approximated by a Gaussian function

$$\delta(x)\approx\frac{1}{\sqrt{\pi}\Gamma}\exp\left(-\frac{x^2}{\Gamma^2}\right). \tag{5}$$

The real part of the dielectric function is obtained from $\epsilon''(\omega)$ by a Kramer–Kronig transformation [9]

$$\epsilon'(\omega) = 1 + \frac{4}{\pi}\mathbf{P}\int_0^\infty d\omega' \frac{\omega'\epsilon''(\omega')}{\omega'^2 - \omega^2}, \tag{6}$$

where **P** denotes the principle value of the integral. Once we get the dielectric function $\epsilon = \epsilon' + i\epsilon''$, linear optical properties, such as refractive index and absorption spectrum, can be calculated.

2.3. Spectral dielectric function at phonon frequencies

The dielectric function in the far-IR band has a different nature, because the dielectric response is determined by the vibrational behavior of ions. Using the response–function formalism within DFT, the second order derivatives of total energy and wave functions of periodic solids with respect to displacement of atoms or homogeneous static electric fields can be calculated [17]. As a result, the parameters such as dynamical matrices, Born effective charges, dielectric permittivity tensors can also be determined. For semiconductors and insulators, the dielectric permittivity tensor is calculated through,

$$D_{\mathrm{mac},a} = \sum_b \epsilon_{\infty,ab} E_{\mathrm{mac},b}, \tag{7}$$

where D_{mac} is the macroscopic displacement field and E_{mac} is the electric field, and a and b denote the directions. Here we use the high frequency dielectric permittivity $\epsilon_{\infty,ab}$ instead of the static dielectric permittivity $\epsilon_{0,ab}$ because in DFT calculations the ions are treated as external potential, and only the electronic contribution is included in polarization.

The knowledge of phonon frequencies and eigenmodes is acquired once dynamical matrix is calculated. Since GaAs is isotropic, the dielectric permittivity tensor reduces to a scalar. The frequency-dependent dielectric function $\epsilon(\omega)$ is calculated by adding the ionic contribution to ϵ_∞ (the oscillator model) [9]

$$\frac{\epsilon(\omega)}{\epsilon_\infty} = 1 + \sum_m \frac{\omega_{\mathrm{LO},m}^2 - \omega_{\mathrm{TO},m}^2}{\omega_{\mathrm{TO},m}^2 - \omega^2 - i\gamma\omega}, \tag{8}$$

where LO and TO denote the longitudinal and transverse optical phonon modes, and m goes over all the IR-active modes. Ab initio calculations are not capable of capturing the temperature-dependent damping term γ in the oscillator model, so it is usually neglected or fitted from experiments [18,19].

2.4. Spectral reflectance

Spectral reflectance of a surface depends on factors including polarization, surface temperature, and surface morphology. To demonstrate our approach, we consider a simple semi-infinite medium at 0 K subjected to normal incidence. Low-temperature assumption indicates that the complicated temperature effects, such as free carrier absorption and electron–phonon coupling, are absent. The complex refractive index $m = n + i\kappa$ is related to the dielectric function through:

$$m^2 = \epsilon = \epsilon' + i\epsilon''. \tag{9}$$

For a perfect surface with normal incidence from vacuum or air, the surface reflectance is given by [20],

$$R = \frac{(n-1)^2 + \kappa^2}{(n+1)^2 + \kappa^2}. \tag{10}$$

3. Results

First-principle calculations are carried out using the plane-wave pseudopotential method, which is implemented in the ABINIT [21] code. Local density approximation (LDA) is used for exchange and correlation potential with Troullier–Martins pseudopotentials [22]. A primitive cell with one Ga and one As atoms and a large plane wave cutoff of 16 Hartree/Bohr are used. A $12 \times 12 \times 12$ k-point grid generated in the irreducible Brillouin zone is used for the k-space integration.

Table 1
The calculated lattice constant and band gap compared with existing experimental and theoretical data.

Parameters	Lattice constant (Å)	Band gap (eV)	Reference
This work	5.45	1.54	
Previous prediction	5.654	1.04	[29]
Experimental data	5.65	1.52	[30]

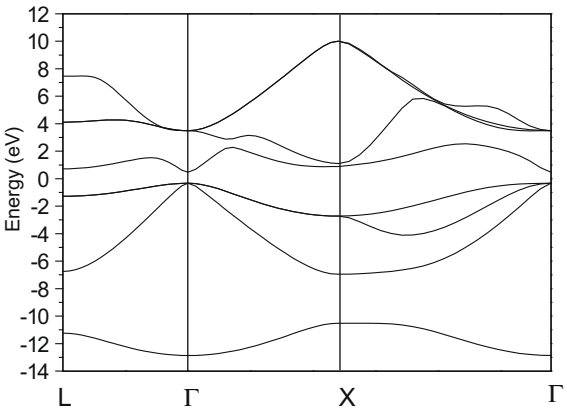

Fig. 1. The calculated electronic band structure of GaAs.

To check the applicability and accuracy of the pseudopotentials, geometry optimization and band structure calculation are first carried out. Since GaAs has a simple zinc-blende structure, the geometry optimization only includes the optimization of lattice constant. The calculated lattice constant and band gap are compared with existing data and listed in Table 1, and the band structure is shown in Fig. 1. The calculated lattice constant is 2% smaller than the experimental value, while the band gap value is similar to experiment. Underestimation of lattice constant is common for GaAs if an LDA based pseudopotential is used without nonlinear-core correction or including d orbitals [23]. Although the lattice constant is underestimated, the standard norm-conserving pseudopotentials give quite decent band structure prediction [23]. Therefore, they are chosen for our calculations.

To obtain the dielectric function within near-IR to UV region, the band structure is analyzed using the ABINIT component OPTIC program, based on Eq. (4). The spectral dielectric function from 0 to 8 eV is shown in Fig. 2. The imaginary part of the dielectric function is zero below 1.54 eV because no absorption occurs below the gap energy. There are three peaks around 3, 5, and 6 eV, which can be attributed to the optical transition near the L and X point in the Brillouin zone [24]. Our prediction matches the second and the third peaks pretty well, while the location and height of the first peak is not well-predicted. The failure to accurately predict the first peak height is also seen in other calculations [25] and is due to the neglecting of excitons.

The calculation of IR permittivity tensor using response–function formalism is also implemented in ABINIT. This approach includes a self-consistent calculation to obtain the charge density, a non-self-consistent calculation to obtain the wave function, and a calculation to generate derivatives of the 1st, 2nd, or 3rd orders with respect to the electric field and the atomic displacement. The static dielectric tensor and dynamical matrices are then ob-

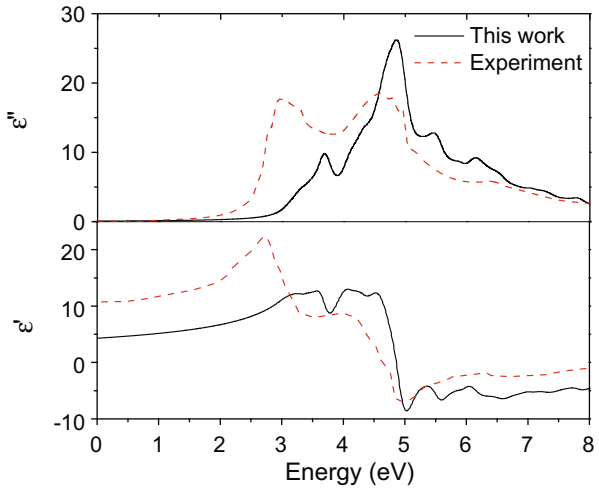

Fig. 2. Our calculated imaginary and real parts of the dielectric function for GaAs from near-IR to UV bands, as compared to experimental data from Ref. [28].

Table 2
The calculated static and high frequency dielectric permittivity and phonon frequencies (with F_2 symmetry) compared with experimental data.

Parameters	ϵ_0, ϵ_∞	F_2(TO,LO) (cm^{-1})	Reference
Our prediction	15.77, 12.85	257.7, 267.5	
Experimental data	13.63, 10.88	271.1, 285.2	[31]

tained. The phonon frequencies and vibrational mode are calculated by diagonalizing the dynamical matrix. The calculated static and high frequency dielectric permittivity and optical phonon frequencies are shown in Table 2. The calculated dielectric permittivity for zero and infinite frequencies are slightly overestimated compared with experimental results, presumably due to the underestimation of the lattice constant. GaAs has a zinc-blende structure, which has only two atoms in a primitive cell and only three optical phonon branches. The calculated zone-center optical phonons frequencies match the experimental value well. Normal mode analysis [11] of zone-center optical phonon indicates that this phonon mode has an F_2 symmetry, which is both Raman and IR active. The photons have much smaller momentum than phonons, so only the interaction with zone-center photon needs to be considered. The spectral dielectric function from 0 to 800 cm^{-1} is then calculated using the oscillator model and shown

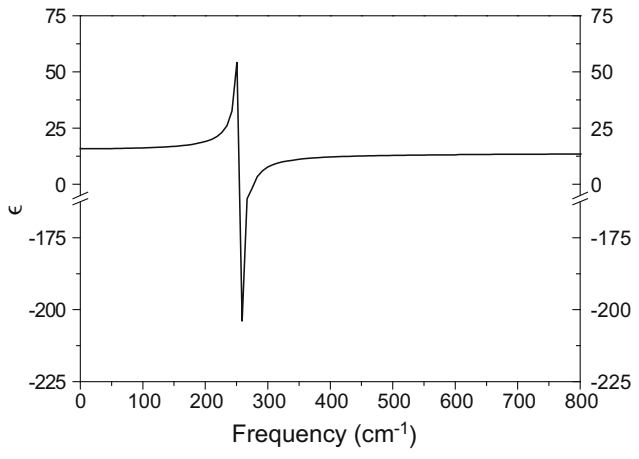

Fig. 3. The calculated IR dielectric function for GaAs.

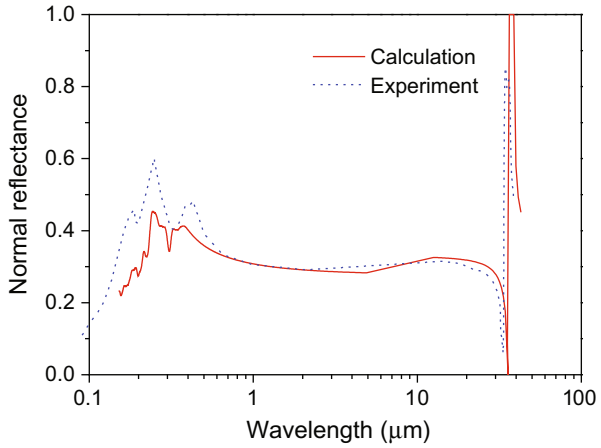

Fig. 4. The calculated reflectance over the entire spectrum compared with experimental data.

in Fig. 3. Damping is neglected here, so the dielectric function is real. Only one peak is observed because there is only one IR-active phonon mode in GaAs.

The calculated reflectance is compared with experimental data [26], as shown in Fig. 4. We choose the low-temperature experimental data because our calculation is performed at 0 K. Overall our data agree well with the experiment. In the IR region, one reflection peak appears which can be attributed to the strong optical phonon oscillation. Compared with the experiment, the calculated reflection peak is higher and reaches one due to the neglect of damping. The reflectance at the plateau between phonon absorption and electron absorption is also similar to experimental results indicating an accurate prediction of high frequency dielectric constant (ϵ_∞). From near-IR to UV range, the reflectance peaks correspond to large interband absorption.

4. Discussions and conclusions

The thermal radiative properties of bulk materials are correlated to their atomic structures, and some general insights can be gained in terms of achieving selective radiative properties. If far-IR absorption is desired, ionic materials should be chosen so that there is dipole in the material that can respond to external field (far-IR light). The absorption peaks are related to the zone-center optical phonon frequencies, which are in turn determined by the bond strength and ion masses. For example, if absorption at lower frequency is needed, materials with heavier atoms and weaker bonds should be considered. If absorption in the visible band is needed, semiconductors are usually used. Chemical bonds in semiconductors are usually not strong so that moderate electronic band gaps are created. Band gap is a very important parameter that determines the onset of the absorption.

After a qualitative understanding of how the atomic structure determines radiative property, our methods described above can be performed to get quantitative results. Although we only calculated the semiconductor GaAs, the numerical method can be further generalized to calculate the dielectric properties of metals and insulators. For metals, the dielectric properties include the free electron contribution and interband transition. The free electron contribution can be well-described by the Drude's model, which requires the electrical conductivity as an input parameter. The interband transition part can be determined by similar ab initio calculations. Because the many-body effect in metals are weaker than in semiconductors, DFT calculations could give even better re-

sults for metals. For insulators, the electronic band gap are usually large, so that usually no interband transition is allowed within visible range. The dielectric function within this frequency is nearly invariant and can be approximated by the high frequency dielectric constant ε_∞. For semiconductors, our method can be further improved by using the GW method to take into account the excitonic effects [27]. For all materials, the phonon contribution part can be calculated using the oscillator model, after the phonon properties are calculated from first-principles.

In summary, the theoretical framework of calculating radiative properties from ab initio methods is presented, using GaAs as an example. Fermi's golden rule is applied to analyze the band structure and determine the spectral dielectric function for near-IR to UV band. Far-IR reflectance is calculated by analyzing the derivatives of energy and wave function with respect to external electric field and atom displacement. This approach can be used to obtain the reflectance using the atomic structure as the only input. Similar calculations can be performed to predict the optical properties of other bulk materials, and some nanostructures such as small nanoparticles.

Acknowledgements

This work is partly supported by the Air Force Office of Scientific Research through the Discovery Challenge Thrust (DCT) Program Grant No. FA9550-08-1-0126 (Program manager: Joan Fuller). H.B. acknowledges the Purdue Computing Research Institute Fellowship. X.L.R. acknowledges the faculty startup fund from Purdue University. Fruitful discussions with Dr. Timothy Fisher are greatly appreciated.

References

[1] K. Watson, S. Ghose, D. Delozier, J. Smith, J. Connell, Transparent, flexible, conductive carbon nanotube coatings for electrostatic charge mitigation, Polymer 46 (2005) 2076–2085.
[2] T. Trupke, E. Daub, P. Wurfel, Absorptivity of silicon solar cells obtained from luminescence, Solar Energy Mater. Solar Cells 53 (1998) 103–114.
[3] A. Narayanaswamy, G. Chen, Thermal emission control with one-dimensional matallodielectric photonic crystals, Phys. Rev. B 70 (2004) 125101.
[4] S. Basu, Y. Chen, Z. Zhang, Microscale radiation in thermophotovoltaic devices – a review, Int. J. Energy Res. 31 (2007) 689–716.
[5] K. Kempa, J. Ryhczynski, Z.P. Huang, K. Gregorczyk, A. Vidan, B. Kimball, J. Carlson, G. Benham, Y. Wang, A. Herczynski, Z.F. Ren, Carbon nanotubes as optical antennae, Adv. Mater. 19 (2007) 421–426.
[6] K. Kempa, B. Kimball, J. Ryhczynski, Z.P. Huang, P.F. Wu, D. Steeves, M. Sennett, M. Giersig, D.V.G.L.N. Rao, D. Carnahan, D.Z. Wang, J.Y. Lao, W.Z. Li, Z.F. Ren, Photonic crystals based on periodic arrays of aligned carbon nanotubes, Nano Letters 3 (2003) 13–18.
[7] V. Yannopapas, Thermal emission from three-dimensional arrays of gold nanoparticles, Phys. Rev. B 73 (2006) 113108.
[8] G. Torsello, M. Lomascolo, A. Licciulli, D. Diso, S. Tundo, M. Mazzer, The origin of highly efficient selective emission in rare-earth oxides for thermophotovoltaic applications, Nat. Mater. 3 (2004) 632–637.
[9] Z.M. Zhang, Nano/Microscale Heat Transfer, McGraw-Hill, New York, 2007.
[10] R. Powell, Physics of Solid-State Laser Materials, Springer, New York, 1998.
[11] D. Rousseau, R. Bauman, S. Porto, Normal mode determination in crystals, J. Raman Spectrosc. 10 (1981) 253–290.
[12] R. Martin, Electronic Structure: Basic Theory and Practical Methods, Cambridge University Press, Cambridge, 2004.
[13] M. Stadele, M. Moukara, J. Majewski, P. Vogl, Exact exchange Kohn–Sham formalism applied to semiconductors, Phy. Rev. B 59 (1999) 10031–10043.
[14] M.C. Payne, M.P. Teter, D.C. Allan, T.A. Arias, J.D. Joannopoulos, Interactive minimization techniques for ab initio total-energy calculations: molecular dynamics and conjugate gradients, Rev. Mod. Phys. 64 (1992) 1045–1097.
[15] R. Hilborn, Einstein coefficients, cross-sections, *f* values, dipole moments, and all that, Am. J. Phys. 50 (1982) 982–986.
[16] G.Y. Guo, K.C. Chu, D.S. Wang, C.G. Duan, Linear and nonlinear optical properties of carbon nanotubes from first-principles calculations, Phys. Rev. B 69 (2004) 205416.
[17] X. Gonze, C. Lee, Dynamical matrices, Born effective charges, dielectric permittivity tensors, and interatomic force constants from density-functional perturbation theory, Phys. Rev. B 55 (1997) 10355–10368.
[18] K. Lee, W.E. Pickett, Born effective charges and infrared response of libc, Phys. Rev. B 68 (2003) 085308.
[19] P. Hermet, M. Goffinet, J. Kreisel, P. Ghosez, Raman and infrared spectra of multiferroic bismuth ferrite from first principles, Phys. Rev. B 75 (2007) 220102.
[20] F. Pedrotti, L. Pedrotti, L. Pedrotti, Introduction to Optics, Pearson Education, New Jersey, 2007.
[21] X. Gonze, J.-M. Beuken, R. Caracas, F. Detraux, M. Fuchs, G.-M. Rignanese, L. Sindic, M. Verstraete, G. Zerah, F. Jollet, M. Torrent, A. Roy, M. Mikami, P. Ghosez, J.-Y. Raty, D. Allan, First-principles computation of material properties: the ABINIT software project, Comput. Mater. Sci. 25 (2002) 478–492.
[22] N. Troullier, J. Martins, Efficient pseudo-potentials for plane-wave calculations, Phys. Rev. B 43 (1991) 1993–2006.
[23] V. Fiorentini, Semiconductor band structures at zero pressure, Phys. Rev. B 46 (1992) 2086–2091.
[24] H. Ehrenreich, H. Philipp, J. Phillips, Interband transitions in groups 4, 3–5, and 2–6 semiconductors, Phys. Rev. Lett. 8 (1962) 59–61.
[25] M.-Z. Huang, W. Ching, Calculation of optical excitations in cubic semiconductors. I. Electronic structure and linear response, Phys. Rev. B 47 (1993) 9449–9463.
[26] Y. Touloukian, D. DeWitt, Thermophysical Properties of Matter, IFI Plenum, New York, 1970–1972.
[27] W.G. Aulbur, L. Jonsson, J.W. Wilkins, Quasiparticle calculations in solids, Solid State Phys. 54 (2000) 1–218.
[28] H.R. Philipp, H. Ehrenreich, Optical properties of semiconductors, Phys. Rev. 129 (1963) 1550–1560.
[29] M.Z. Huang, W. Ching, A minimal basis semi-ab initio approach to the band structures of semiconductors, J. Phys. Chem. Solids 46 (1985) 977–995.
[30] C. Kittel, Introduction to Solid State Physics, Wiley, New York, 1996.
[31] J. Blakemore, Semiconducting and other major properties of gallium arsenide, J. Appl. Phys. 53 (1982) R123–R181.